Royal College of Surgeons in Ireland

repository@rcsi.com

# Hypoxia-mimicking bioactive glass/collagen glycosaminoglycan composite scaffolds to enhance angiogenesis and bone repair.

AUTHOR(S)

Elaine Quinlan, Sonia Partap, Maria M. Azevedo, Gavin Jell, Molly M. Stevens, Fergal O'Brien

CITATION

Quinlan, Elaine; Partap, Sonia; Azevedo, Maria M.; Jell, Gavin; Stevens, Molly M.; O'Brien, Fergal (2015): Hypoxia-mimicking bioactive glass/collagen glycosaminoglycan composite scaffolds to enhance angiogenesis and bone repair.. Royal College of Surgeons in Ireland. Journal contribution. https://hdl.handle.net/10779/rcsi.10766375.v1

HANDLE

10779/rcsi.10766375.v1

LICENCE

CC BY-NC-SA 4.0

This work is made available under the above open licence by RCSI and has been printed from https://repository.rcsi.com. For more information please contact repository@rcsi.com

URL

https://repository.rcsi.com/articles/journal_contribution/Hypoxia-mimicking_bioactive_glass_collagen_glycosaminoglycan_composite_scaffolds_to_enhance_angiogenesis_and_bone_repair_/10766375/1

# Hypoxia-Mimicking Bioactive Glass/Collagen Glycosaminoglycan Composite Scaffolds to Enhance Angiogenesis and Bone Repair

Quinlan, E.,[1,2,3†] Partap, S.,[1,2†] Azevedo, M.M.,[4,5] Jell, G.,[4,5] Stevens, M.M.[4,5] & O'Brien, F.J.[1,2,3*]

[1]Department of Anatomy, Royal College of Surgeons in Ireland, Dublin 2, Ireland,

[2]Trinity Centre for Bioengineering, Department of Mechanical Engineering, Trinity College, Dublin 2, Ireland

[3]Advanced Materials and BioEngineering Research Centre (AMBER), RCSI & TCD, Dublin 2, Ireland,

[4]Department of Materials, Imperial College London, London SW7 2AZ, UK

[5]Institute for Biomedical Engineering, Imperial College London, London SW7 2AZ, UK

[†]These authors contributed equally.

**Address Correspondence and Reprints Requests to:*

Prof. Fergal J. O'Brien

Department of Anatomy

Royal College of Surgeons in Ireland

123 St. Stephen's Green

Dublin 2

Ireland

Phone: +353-(0)1-402-2149

Fax: +353-(0)1-402-2355

Email: fjobrien@rcsi.ie

**Abstract**

One of the biggest challenges in regenerative medicine is promoting sufficient vascularisation of tissue-engineered constructs. One approach to overcome this challenge is to target the cellular Hypoxia Inducible Factor (HIF-1α) pathway, which responds to low oxygen concentration (hypoxia) and results in the activation of numerous pro-angiogenic genes including vascular endothelial growth factor (VEGF). Cobalt ions are known to mimic hypoxia by artificially stabilising the HIF-1α transcription factor. Here, resorbable bioactive glasses particles (38 μm and 100 μm) with cobalt ions incorporated into the glass network were used to create bioactive glass -collagen–glycosaminoglycan scaffolds optimised for bone tissue engineering. Inclusion of the bioactive glass improved the compressive modulus of the resulting composite scaffolds while maintaining high degrees of porosity (>97%). Moreover, *in vitro* analysis demonstrated that the incorporation of cobalt bioactive glass with a mean particle size of 100μm significantly enhanced the production and expression of VEGF in endothelial cells, and cobalt bioactive glass/collagen–glycosaminoglycan scaffold conditioned media also promoted enhanced tubule formation. Furthermore, our results prove the ability of these scaffolds to support osteoblast cell proliferation and osteogenesis in all bioactive glass/collagen–glycosaminoglycan scaffolds irrespective of the particle size. In summary, we have developed a hypoxia-mimicking tissue-engineered scaffold with pro-angiogenic and pro-osteogenic capabilities that may encourage bone tissue regeneration and overcome the problem of inadequate vascularisation of grafts commonly seen in the field of tissue engineering.

**Keywords:** Collagen; Scaffold; Bioactive Glass; Cobalt; Angiogenesis; Regenerative Medicine

## 1. Introduction

For bone repair, the surgeons preferred choice of a bone substitute remains the bone graft, specifically the autograft, creating an elevated demand for these materials worldwide. The main disadvantage associated with this approach is the requirement of an extra surgery to harvest the autologous bone, and the pain associated with the harvest site is often said to be more painful than the recipient site [1]. Hence, the field of regenerative medicine aims to address this issue by developing new substitutes that can activate the body's own natural repair process omitting the need for donor tissue [2]. Scaffolds provide sites for cell attachment, mechanical stability within the defect site, and a porous and interconnected pore network for interaction with the host (for cell migration, and nutrient and waste removal) [3]. In our laboratory, we have developed a series of scaffolds from type I collagen and the abundant polysaccharide, glycosaminoglycan, to produce highly porous collagen–glycosaminoglycan (CG) scaffolds by using a controlled freeze-drying process [4-6]. These scaffolds have an optimised composition to facilitate osteogenesis [7] and have been shown to enhance bone repair *in vivo* in minimally loaded calvarial defects [8-10].

The traditional role of the scaffold as simply a template for tissue formation has evolved and the new generation of scaffolds are increasingly being used as delivery vehicles for therapeutic molecules such as drugs, proteins and genes that initiate biological events leading to the regeneration of tissue [5]. Ions can also be classified as therapeutics; for instance, it has been shown that silicon (Si) and calcium (Ca) ions initiate osteogenesis when released in biologically relevant ranges (15–30 ppm for Si and 60–90 ppm for Ca) [11, 12]. One method of delivery is the release of Si and Ca ions from bioactive glasses, which are defined as inorganic surface-active bioceramics. When exposed to biological fluids, bioactive glasses form a hydroxyl carbonate apatite layer; this layer then forms a bond between the bioactive glass and bone, imparting pro-regenerative ability to the bioactive glass allowing for bone ingrowth [11]. An approach to further enhance the therapeutic potential of the bioactive glass is to introduce ions such as strontium [13], magnesium or zinc [14], which are known to have anabolic responses in bone metabolism. Controlled rates of dissolution of the bioactive glass provide the physiologically relevant concentrations of the biologically active ions to the cells when exposed to body fluids [11]. 45S5 Bioglass particles, NovaBone and PerioGlas are examples of commercially available bioactive glass products that are used in the treatment of a wide range of dental and orthopaedic diseases [15].

One of the biggest challenges faced in the field of regenerative medicine is promoting the growth of vasculature within engineered tissues to enable sufficient engraftment and integration

within the host [16]. Lack of vascularisation can lead to graft failure due to avascular necrosis. Methods of initiating angiogenesis include using expensive recombinant pro-angiogenic vascular endothelial growth factor (VEGF) proteins and genes encoding for VEGF. However, these approaches have had limited success due to the uncontrolled manner in which proteins are released, high doses of protein required, short protein half-life, low transfection efficiencies associated with gene-based approaches and potential safety concerns within a clinical setting [17, 18]. Furthermore, single growth factor release has previously been shown to lead to the formation of immature vasculature [19]. An alternative strategy is to target the cellular Hypoxia Inducible Factor (HIF-1α) pathway, which responds to low oxygen concentration (hypoxia) and results in the activation of a cascade of pro-vasculogenic genes critical for angiogenesis, including VEGF mimicking the normal regenerative response [20]. Cobalt ions ($Co^{2+}$) have the potential to mimic hypoxia, they artificially stabilise the transcription factor HIF-1α [20, 21], which then translocates into the nucleus to stimulate the upregulation of pro-vasculogenic genes such as VEGF [22]; this approach has been adopted as a potential neovascularisation strategy in a number of studies [23, 24]. Recently, cobalt-releasing bioactive glasses have been developed [25], and their ability to activate the HIF pathway under normoxic conditions was demonstrated [26].

The focus of this study was to incorporate cobalt bioactive glass [25] into CG scaffolds that have been developed and optimised for bone tissue regeneration [7, 27-29] with a view to improving the mechanical and structural properties of the CG scaffold and, most importantly, enhancing the initial angiogenic step vital for bone regeneration [30, 31]. Specifically, the aims were to assess the effect of the bioactive glass on the pore structure, porosity, compressive moduli and biological activity of the resultant composites by examining their ability to induce an angiogenic and osteogenic response from cells.

## 2. Materials and Methods

### 2.1 Synthesis of bioactive glass

Bioactive glasses were synthesised in the Stevens's laboratory in Imperial College London. A series of bioactive glasses containing either no cobalt or 4 mole% cobalt were prepared by the melt-quench route as previously described [25]. The resulting powder was sieved to obtain particle sizes with a mean diameter of 38 μm and 100 μm.

## 2.2 Scaffold fabrication

A CG slurry was produced by mixing type I collagen (1.8 g) isolated from bovine tendon (Integra, New Jersey, USA) in 300 mL aqueous 0.5 M glacial acetic acid solution, followed by the dropwise addition of 0.32 g of the glycosaminoglycan chondroitin-6-sulphate sodium salt (Sigma-Aldrich, Ireland) dissolved in 60 mL of 0.5 M aqueous acetic acid solution [4]. The slurry was then degassed for a few hours. For the composites, three different types of bioactive glass were investigated: (1) cobalt-free with an average particle diameter of 38 μm; (2) cobalt bioactive glass with an average particle diameter of 38 μm; and (3) cobalt bioactive glass with an average particle diameter of 100 μm. The cobalt bioactive glasses had a concentration of 4 mole% cobalt. The bioactive glass was suspended in distilled water at a concentration of 0.14 g/mL. Various volumes (0.5, 0.2 and 0.1 mL) of the bioactive glass suspension were added dropwise to 20 mL of the CG slurry. The slurries were homogenised at a low speed to ensure a homogeneous distribution of the bioactive glass, however, even at this low speed, excess air could be incorporated during the addition. At this stage, either the slurry was degassed a second time to remove excess air or the slurry was immediately frozen in a controlled manner.

For the latter process, 2 mL of the slurry was pipetted immediately into each well of a 24-well plate and lyophilised (Advantage EL, VirTis Co., Gardiner, NY) for 24 h using a final freezing temperature of –40°C. Initial freezing rates of either $1^{o}$C/min or $4^{o}$C/min were investigated. A range of scaffolds were fabricated by this method with final concentrations of 0, 1.4, 2.8 and 7 mg of bioactive glass per scaffold.

All scaffold variants were sterilised after fabrication using a dehydrothermal treatment for 24 h at 105 °C and then further chemically crosslinked using 14 mM *N*-(3-dimethylaminopropyl)-*N*'-ethylcarbodiimide hydrochloride) and 5.5 mM *N*-hydroxysuccinimide (Sigma-Aldrich, Ireland) in distilled water for 2 h followed by 2 x 30 min rinses in phosphate buffered saline (PBS) [28].

## 2.3 Physical characterisation of bioactive glass/CG scaffolds

### 2.3.1 Release of cobalt from scaffolds

Ion Chromatography Plasma Mass Spectrometry (ICP-MS) was employed. Scaffolds were incubated in 5 mL TRIS buffer that was completely replaced at 24 h and then again at 7 days. TRIS buffer collected at the 24 h and 7 day time points were frozen at $–80^{o}$C until analysis. ICP-MS was performed on a Varian 8200 machine. All samples were run in triplicate.

### 2.3.2 Effect of bioactive glass incorporation on scaffold mechanical properties

Compressive modulus of the scaffolds was determined using a Z050 mechanical testing machine (Z050, Zwick/Reoll) fitted with a 5-N load cell. Unconfined, wet compression testing was performed on 9-mm-diameter scaffolds with a thickness of 6–7 mm that were immersed in PBS and tested at a rate of 10% strain per min. The modulus was calculated from the slope of the stress–strain curve over the range 2–5% strain ($n$ = 4).

### 2.3.3 Effect of bioactive glass incorporation on scaffold porosity

Scaffolds were embedded in JB4 glycomethacrylate resin according to manufacturer's instructions (Polysciences, Germany). The embedded scaffolds were sectioned at 10 μm thicknesses (Leica RM 2255, Leica, Germany microtome). The sections were mounted on slides and then stained with an aqueous 1 wt% Toludine Blue solution for 5 min. The slides were rinsed in distilled water and left to dry, then were mounted with coverslips using DPX mountant. The sections were imaged using a Nikon microscope (Optimphot2, Nikon, Japan). The pore diameters were determined from the images using MatLab pore topology analyser software as previously described [4].

The porosity of the scaffolds with and without bioactive glass was calculated using the following equation:

$$\% \text{ porosity} = 100 \times [1 - (\rho_{actual}/\rho_{theoretical})]$$

The actual density ($\rho_{actual}$) of the scaffolds was calculated by dividing the actual mass of the scaffolds by the volume of the scaffolds which was then divided by the theoretical density ($\rho_{theoretical}$) of the materials.

## 2.4 Biological response of bioactive glass/CG scaffolds

### 2.4.1 Cell culture and seeding

To assess the angiogenic and osteogenic response of the scaffolds, two commonly used cell lines were employed: (1) Human Umbilical Vein Endothelial Cells (HUVECs) were cultured to confluence in complete endothelial media (EGM-2, Lonza, UK) in T175 flasks (Sarstedt, Dublin, Ireland) under standard conditions (37$^{o}$C, 5% $CO_2$); (2) MC3T3-E1 cells, from a pre-osteoblastic cell line, were cultured to confluence in standard α-minimum essential medium (MEM) supplemented with 10% fetal bovine serum (FBS), 15 L-glutamine and 2% penicillin/streptomycin. Prior to seeding the cells were detached from the flasks using trypsin-

EDTA (Sigma-Aldrich, Dublin, Ireland) and suspended in media to obtain a final concentration of 10 x $10^6$ cells per mL. In a 24-well plate, each scaffold was seeded dropwise with 25 µL of the cell suspension and then placed in the incubator for 15 min, the scaffolds were then turned over and another 25 µL of the cell suspension was added dropwise (total number of cells per scaffold = 5 x $10^5$ cells) to produce a cell-seeded construct. After 15 min, 2 mL of either endothelial media (for HUVECs) or osteogenic media (for MC3T3-E1 cells; α-MEM supplemented with 50 µM ascorbic acid 2-P, 100 nM dexamethasone, 10 mM β-glycerophosphate, 10% FBS, 100 U/mL penicillin, 100 µg/mL streptomycin) was added to each well and the scaffolds returned to the incubator. The constructs were cultured for 24 h, 3 and 7 days in the case of HUVECs and for 3, 7, 14 and 28 days in the case of MC3T3-E1 cells to allow for mature osteogenesis to take place. At each timepoint, constructs were rinsed twice in PBS, flash frozen using liquid nitrogen and stored at –80$^o$C until analysis of RNA and DNA content. One scaffold was fixed in 10% formalin for histological analysis. Additionally, 1 mL of supernatant was collected and stored at –80 $^o$C until analysis by enzyme-linked immunosorbent assay (ELISA).

### 2.4.2 Analysis of angiogenesis in bioactive glass/CG scaffolds

**DNA quantification**

Those scaffolds that were flash frozen were digested in lysis buffer containing 1% β-mercaptoethanol in RLT buffer (Qiagen RNeasy kit, Qiagen, Ireland) and homogenised using a rotor-stator homogeniser (Omni International, Germany) and subsequently analysed for DNA content as a marker for cell proliferation. Cell lysates were centrifuged using QIA shredder columns (Qiagen, Ireland) to remove any scaffold material. The subsequent sample was then analysed using the PicoGreen assay according to the manufacturer's protocol (Quanti-iT PicoGreen dsDNA Molecular Probes, OR, USA).

**VEGF gene expression**

RNA extraction was carried out using the RNeasy Mini Kit (Qiagen, Ireland) according to the manufacturer's protocol. Expression levels of the angiogenic marker VEGF were investigated using quantitative real-time polymerase chain reaction (RT-PCR). Reverse transcriptions (20 µl) were performed on 100 ng of total RNA using the QuantiTect Reverse Transcription Kit according to the manufacturer's instructions. Real-time PCR reactions (15 µl) were performed in triplicate on a 7500 Real-Time PCR system (Applied Biosystems, Foster City, CA, USA) using the QuantiTect SYBR Green PCR kit (Qiagen, Ireland). The two predesigned human primers

(Qiagen, QuantiTect Primer Assays) that were used were VEGF primer (Hs_VEGFA_6_SG) and the housekeeping gene 18s primer (Hs_RRN18S_1_SG). Relative expression of VEGF was determined using the ΔΔCT method [32].

**VEGF protein production**

Media samples were analysed using a VEGF ELISA (Quantikine ELISA kit, R&D Systems, Europe) according to the manufacturer's instructions.

**Matrigel assay**

A tubule-forming assay was performed to assess the ability of cobalt released from the cobalt bioactive glass/CG scaffold to promote angiogenesis. Briefly, Matrigel™, a basement membrane matrix commonly used to observe *in vitro* angiogenesis, was placed in a 12-well plate at 300 µL/well. HUVECs were then plated at a density of $9 \times 10^4$ cells per well. Plates were placed in an incubator for 20 min after which time 1 mL of endothelial media (without VEGF supplement) was added. Transwell inserts containing bioactive glass-free CG and cobalt bioactive glass/CG scaffolds were applied on top of the wells. A further 1 mL of media was then added to the wells containing the scaffolds. Matrigel cultures were imaged at 6, 12 and 24 h with a Leica DMIL microscope (10x objective, DFC420C digital camera). For each group, 5 images were taken and analysed using ImageJ. The length of the tubules was used as a quantitative measure of angiogenesis.

**2.4.3 Analysis of osteogenesis in bioactive glass/CG scaffolds**

**DNA and alkaline phosphatase quantification**

DNA content was assessed as described previously. Alkaline phosphatase (ALP) activity was assessed at day 7 to demonstrate the ability of the scaffolds to support osteogenesis. At the endpoint of the study constructs containing MC3T3-E1 cells were washed in PBS and lysed according to the manufacturer's protocol (SensoLyte pNPP Alkaline Phosphatase Assay Kit). Briefly, scaffolds were homogenised in the appropriate lysis buffer and incubated at 4 ºC. This method utilized *p*-nitrophenyl phosphate (pNPP) that is hydrolysed by ALP to produce a yellow product. The amount of coloured product is proportional to the amount of enzyme in the reaction.

**Cell-mediated mineralisation**

To assess cell-mediated matrix mineralisation on the scaffolds in response to cobalt-free bioactive glass and cobalt bioactive glass, three different methods were used; alizarin red and von Kossa staining, as well as calcium quantification (at day 28). To examine the ability of the constructs to produce calcium phosphates, wax-embedded scaffold sections (10 μm) were de-paraffinized to distilled water and stained with (1) 2% alizarin red (Sigma-Aldrich, Ireland) for 2 min and then mounted with a coverslip or with (2) 2% silver nitrate solution and exposed to ultraviolet light for 20 min prior to mounting. Digital images were obtained as previously described. The ability of the bioactive glass-containing CG scaffolds — both cobalt-free and cobalt bioactive glasses — to induce mineralisation by pre-osteoblasts was further assessed using a calcium quantification technique used routinely in our laboratory [4, 5, 7, 8, 28, 29]. Constructs were added to 1 mL of 0.5 M hydrochloric acid, homogenised using a rotor-stator homogeniser and incubated overnight at 4 ºC whilst shaking to disassociate calcium from proteins. The samples were analysed according to the StanBio Calcium Liquicolour Kit 0150 assay protocol. A standard curve was constructed from 0 to 1 μg/mL, and from the equation of the trendline the concentration of calcium per sample was obtained.

**2.5 Statistical analysis**

Data are represented as mean ± standard deviations. Statistics were carried out using a GraphPad Prism software using a general linear model ANOVA with Tukey's post hoc tests performed for multiple comparisons. All cell cultures were performed with a sample size of 3 per treatment group. Statistical significance was taken at $p<0.05$ unless otherwise stated.

**3 Results**

**3.1 Scaffold fabrication**

A series of preliminary experiments were conducted to establish the optimal scaffold fabrication process for the successful introduction of bioactive glass into CG scaffolds. It was observed that for all scaffold types the faster cooling rate (4$^{o}$C/min) produced a thin film on the scaffold surface that could potentially be problematic for cell attachment and infiltration; furthermore a heterogeneous pore structure was observed compared with that seen in scaffolds made with the slower cooling rate of 1$^{o}$C/min (Fig. 1). Moreover, the initial analysis (supplementary information) showed that the length of time the bioactive glass was in contact with the acidic collagen slurry affected the resulting freeze-dried scaffold structure; the addition

of the bioactive glass caused the pH of the slurry to increase, causing it to separate. Thus, the optimal scaffold fabrication process to reduce this effect and maintain the microstructural integrity was determined to be the addition of bioactive glass into the pre-formed CG slurry (which was degassed prior to the addition to remove air bubbles) followed by freeze-drying at a cooling rate of $1^{o}$C/min for 24 h at a final freezing temperature of –40°C. These studies resulted in a fabrication process that could consistently produce homogenous bioactive glass-containing CG scaffolds.

### 3.2. Physical characterisation of bioactive glass/CG scaffolds

#### 3.2.1 Release of cobalt from scaffolds

Only the composites containing 2.8 and 7 mg of cobalt bioactive glass per scaffold released cobalt ions in the biologically relevant range of 3–12 ppm sufficient for activation of the HIF-1α pathway [25, 33]. However, only those that incorporated 7 mg of bioactive glass per scaffold released >3 ppm of cobalt at each of the timepoints examined (day 3 and 7; Fig. 2). The ability of the two different sized cobalt bioactive glasses to release cobalt ions at different rates based on their varying surface-area-to-volume ratios was investigated. It was observed that the particle size of the bioactive glass did not significantly affect the release behaviour of cobalt ions (Fig. 2) although smaller particles (38 μm) displayed a trend towards increased ion release at both timepoints.

#### 3.2.2 Effect of bioactive glass incorporation on scaffold mechanical properties

A series of tests were conducted to examine the effects of bioactive glass on the physical characteristics of the scaffolds. The compressive moduli of the scaffolds were significantly increased by the addition of bioactive glass when compared with the negative control (bioactive glass-free CG scaffold; Fig. 3A) showing that the particles reinforce the scaffolds. It was also observed that the moduli increased with increasing bioactive glass concentration (data not shown). All further *in vitro* studies were carried out with the composite containing 7 mg of bioactive glass per scaffold, which was deemed to be most optimal based on the cobalt release kinetics and improved mechanical properties.

#### 3.2.3 Effects of bioactive glass incorporation on scaffold porosity

Scaffold porosity reduced as a result of the incorporation of bioactive glass compared with the control, but was maintained at levels beneficial for cellular and vascular infiltration, and

tissue growth. All scaffolds maintained high degrees of porosity of 98% and above (Fig. 3B). The scanning electron micrographs in Figure 3C show the highly porous architecture of the scaffolds, and an even distribution of bioactive glass was observed throughout the collagen matrix.

### 3.3 Effect of bioactive glass incorporation on biological response

#### 3.3.1 Analysis of angiogenesis in bioactive glass/CG scaffolds

To investigate cellular interactions, HUVECs were seeded onto the optimised scaffolds (containing 7 mg of bioactive glass per scaffold). Initially, a reduction in cell number was observed on scaffolds containing cobalt-free bioactive glass at day 1 and day 3 compared with all other groups. However, by day 7, cell numbers were relatively homogenous for the different composites examined. There was no significant drop in cell number for scaffolds with the cobalt bioactive glass (Fig. 4A) across the time period examined. VEGF gene expression was upregulated for scaffolds with cobalt bioactive glass (Fig. 4B). Initially, the smaller-diameter cobalt bioactive glass particles showed higher levels after 24 h and 3 days, but by day 7 the highest gene expression was observed for scaffolds with the larger-diameter particles. Furthermore, VEGF gene expression correlated with VEGF protein production (Fig. 4C) where, by day 7, the highest levels of protein were seen for scaffolds with the larger-diameter particles. The ability of the cobalt bioactive glass/CG scaffolds to promote tubule formation with HUVECs was then assessed using a tubule-formation assay (Fig. 4D). It was observed that HUVECs cultured with the dissolution media from cobalt bioactive glass/CG scaffolds displayed enhanced vascular tubule formation compared with the bioactive glass-free CG control (Fig. 4D, E) at 4 and 12 h, further indicating a cobalt bioactive glass-induced angiogenic response. Tubule formation was more enhanced in the presence of larger-diameter cobalt bioactive glass particles of 100 μm compared with the smaller particles with a mean diameter of 38 μm (Fig. 4E), which corroborated the gene and protein data.

#### 3.3.2 Analysis of osteogenesis in bioactive glass/CG scaffolds

When pre-osteoblastic cell number was assessed as a marker for cell proliferation, there was no significant reduction in the presence of bioactive glass (Fig. 5A) compared with the bioactive glass-free CG scaffold from day 3 to day 7. At day 14 the CG scaffold alone had the highest cell numbers but by day 28 there was no difference in cell numbers on the different

scaffolds. Cell numbers increased to a similar extent as the control from day 3 through to day 28 indicating cellular activity on the scaffolds in the presence of bioactive glass. The osteogenic activity of these cells was then measured by monitoring ALP production at day 7. Significant effects of the incorporation of cobalt bioactive glass were observed at day 7 ($p<0.05$). Importantly, ALP activity was upregulated (2.6 and 2.2 fold) in the presence of cobalt-eluting bioactive glass particles (100 μm and 38 μm, respectively) compared with the CG scaffold. Interestingly, cobalt-eluting bioactive glass also promoted enhanced ALP activity compared with the cobalt-free bioactive glass/CG scaffold, suggesting a cobalt bioactive glass-induced osteogenic response (Fig. 5B). Similarly alizarin red staining of scaffolds that had been cultured for 28 days revealed enhanced calcium deposition within the bioactive glass/CG scaffolds compared with the CG scaffold alone (Fig. 5C). Cell-mediated calcium production from cells seeded on the scaffolds for a period of 28 days was next quantified (Fig. 5D). The results corroborated the histological results. Increased calcium deposition was reported in scaffolds containing cobalt-free bioactive glass ($p<0.001$; 38 μm) and, to a lesser extent cobalt-eluting bioactive glass. A significant increase was observed in the scaffolds containing smaller cobalt bioactive glass particles (38 μm) compared with the CG control. Taken together, cobalt bioactive glass/GC composite scaffolds were shown to enhance angiogenic activity and influence osteogenesis.

## 4. Discussion

One of the main limitations in regenerative medicine is achieving functionally vascularised constructs that can integrate fully with the host tissue on implantation [16]. Conventional approaches involving the delivery of therapeutic growth factors aimed at initiating angiogenesis and osteogenesis [34] have many limitations leading to potential safety concerns within a clinical setting [17]. The focus of this study was to combine resorbable bioactive glasses with hypoxia-mimicking cobalt ions with a CG scaffold optimised for bone tissue regeneration. The results confirmed the potential of CG scaffolds incorporating cobalt bioactive glass as a biomaterials-based approach for bone repair. Inclusion of the cobalt bioactive glass not only improved the compressive modulus of the composite scaffolds and maintained high degrees of porosity, but it also induced an angiogenic influenced the osteogenic response from endothelial and pre-osteoblastic cells, respectively. These composite scaffolds may have significant potential in bone tissue regeneration applications negating the need for growth factors, which are often expensive, have disputed efficacy and are often associated with non-specific target effects.

The development of a fabrication process that could consistently produce homogenous cobalt bioactive glass/CG scaffolds was a significant challenge. Bioactive glass stimulates bone bonding by forming a hydroxyl carbonate apatite (HCA) layer on the glass surface following contact with biological fluid thereby stimulating osteogenesis. The HCA layer is formed as a result of a sequence of chemical events that are initiated in the presence of biological fluids. The first step is the rapid exchange of $Na^+$ and $Ca^{2+}$ with $H^+$ or $H_3O^+$ from the solution, causing hydrolysis of the silica groups in the bioactive glass to create silanols. However, the pH of the solution increases as a result of the $H^+$ ions in the solution being replaced by cations [35]. In this study, this initial increase in pH due to cation exchange caused some difficulties for the incorporation of the bioactive glass into the CG slurry. Thus, the challenges were to (1) incorporate the bioactive glass and (2) to minimise the length of time it spent in the slurry to prevent the pH increasing and the slurry subsequently separating. Immediate freezing at a controlled cooling rate of $1^oC$/min was found to be optimal as this regime produced a homogenous distribution of bioactive glass and pore structure. Previous work has combined bioactive glass with collagen sponges via a soak loading method [36], however, directly incorporating bioactive glass into a preformed collagen slurry followed by lyophilisation to yield a microparticle-loaded scaffold has thus far never been successfully achieved to the best of our knowledge. Yet, despite the aforementioned limitations we successfully developed a method to fabricate collagen-based scaffolds incorporating cobalt bioactive glass using a lyophilisation technique.

The addition of bioactive glass led to improved mechanical properties. Higher compressive moduli were observed with increasing amounts of bioactive glass as a result of the reinforcing effect of the particles within the scaffold framework. This effect has previously been demonstrated in our laboratory where it has been shown that the incorporation of ceramic particles into collagen-based scaffolds led to improved mechanical properties [37, 38]. Encouragingly, the addition of the bioactive glass did not affect porosity of the CG scaffold; all composite scaffolds had porosities above 98%, a level that has been shown to be suitable for cellular and vascular infiltration of scaffolds [8].

The majority of research pertaining to the ability of bioactive glass to induce an angiogenic or osteogenic response has been carried out on the soluble dissolution products of bioactive glass as reviewed by Hoppe *et al*. [11]. However, we sought to investigate the effects of cells cultured in direct contact with these materials. Previous work has shown that incorporating cobalt into mesoporous bioactive glasses represents a viable option for promoting enhanced

angiogenesis using human bone marrow stromal cells [39]. Because high concentrations of cobalt ions may cause cell toxicity the controlled release of cobalt ions from bioactive glass is therefore desirable at concentrations pertinent to HIF-1α stabilisation. Scaffolds containing 7 mg bioactive glass per scaffold released cobalt ions within the biologically active concentration range of 3–12 ppm. This range was previously determined to promote angiogenesis *in vitro* using endothelial cells [22, 33, 40] and *in vivo* [21], well below cytotoxic levels [39, 41].

Thus, these scaffolds (containing 7 mg BG per scaffold) were further analysed *in vitro* to assess their ability to promote VEGF gene and protein production as well as tubule formation. The mechanism of angiogenesis is coordinated by genes encoding for cytokines and growth factors such as VEGF. VEGF has been implicated as a critical regulator of neovascularisation [42] and is also fundamental to the osteogenic response in bone healing where it is essential for intramembranous and endochondral bone formation [43]. VEGF gene expression at days 1 and 3 was initially higher in scaffolds containing smaller (38 μm) bioactive glass particles compared with the bioactive glass-free CG control and the scaffold with larger particles (100 μm). However, by day 7 VEGF gene expression was significantly upregulated in HUVECs cultured on scaffolds containing the larger particles (100 μm). Hypoxia, via the HIF pathway mediates a broad range of Hypoxia Responsive Element genes  important in regeneration, including a number of angiogenic such as VEGF [44]. Cobalt bioactive glasses have previously been shown to mimic hypoxia by artificially stabilising HIF-1α leading to enhanced VEGF expression, however, a different cellular model that used mesenchymal stem cells was used [26].

Encouragingly, VEGF gene expression results were further corroborated by the observation of enhanced VEGF protein secretion from cells cultured on bioactive glass-containing scaffolds. Those containing 100-μm-sized particles were found to significantly upregulate VEGF protein production (0.5-fold increase) compared with the smaller particles after 7 days of culture. Further, enhanced tubule formation with a more pronounced tubule length was demonstrated in scaffolds containing larger particles compared with those containing smaller particles and the bioactive glass-free scaffold at 4 h. The different patterns of VEGF gene and protein production between the differently sized bioactive glass particles may be attributed to the expected different cobalt release profiles, with smaller particles (38 μm) having a larger surface area and therefore eluting cobalt (and other ions) at a faster rate than larger particles (100 μm), however, no significant differences in cobalt ion release was observed. Lower concentrations of cobalt released from the larger particles at later timepoints may be more beneficial than high cobalt concentrations eluted from smaller particles. VEGF protein levels were shown to decrease

with time in the bioactive glass-free CG scaffolds whereas enhanced protein secretion was recorded from day 3 to 7 in the bioactive glass-loaded scaffolds. The half-life of endogenous VEGF mRNA increases during hypoxia [45] and this may explain why VEGF protein accumulates with time in cells exposed to cobalt-containing composite scaffolds. Therefore, these results indicate that the composite scaffolds initiate a cobalt-induced pro-angiogenic response. Some studies suggest that particular compositions of bioactive glass itself indirectly enhances angiogenesis, as reviewed elsewhere [46], an effect that was not observed in this study for either gene or protein production (data not shown). However, this effect occurs over a very limited range of compositions of bioactive glasses with as of yet uncharacterized outcomes [47].

CG scaffolds [4, 6] have previously been developed to serve as analogues of native extracellular matrix [8, 48] for bone repair. However, we hypothesised that in addition to enhancing the angiogenic potential of the scaffolds, the osteogenic abilities of the CG scaffold may also be improved by the bioactive glass as it well known to have excellent osteoconductive and osteoinductive properties [49, 50]. Bioactive glass has shown considerable potential in actively promoting osteoblast differentiation via the induction of phenotypic markers such as ALP [51-53]. Microarray analysis has also confirmed that solutions containing phosphate, silicon and calcium, the primary ionic dissolution products of bioactive glass, are capable of directly inducing genes relevant to osteoblast metabolism and the maintenance of extracellular matrix [53]. With this in mind the osteogenic potential of the bioactive glass/CG scaffolds was investigated by examining the ability to induce growth and differentiation of MC3T3 pre-osteoblast-like cells. Cell number was shown to be significantly reduced in the presence of bioactive glass. Ion-induced cell death such as from calcium ions [54] may account for the reduced cell numbers due to the initial ion release from the bioactive glass causing a change in the pH of the surrounding media, an effect that could be minimized in the *in vivo* environment. ALP, an early marker for osteogenic differentiation, was significantly increased in cells cultured on scaffolds containing cobalt-eluting bioactive glass particles (irrespective of particle size) compared with the bioactive glass-free CG scaffold and the cobalt-free bioactive glass-containing scaffold. The calcium quantification results further show that scaffolds containing bioactive glass were capable of promoting differentiation of pre-osteoblasts to a mature mineral depositing osteoblast. Calcium deposition was the highest in the presence of cobalt-free bioactive glass and less pronounced with cobalt bioactive glass. Thus, CG scaffolds, containing cobalt bioactive glass particles, may potentially provide a better environment for bone tissue formation or

biosynthesis compared with the traditional CG scaffold both in terms of enhancing cell-mediated osteogenesis as well as being mechanically superior.

The delivery of tissue-inductive factors in the form of cobalt bioactive glass, from an osteoconductive substrate such as CG scaffolds, offers considerable potential for enhanced bone tissue repair and regeneration. The importance of the interplay between angiogenesis and bone formation has previously been reported with several studies suggesting the synergism between the two processes leads to increased bone healing [55]. The presentation of multiple regulatory signals is essential for many tissue regeneration processes and may thus be a prerequisite for the design of more advanced tissue-engineered materials.. Taken together, the results indicate for the first time that hypoxia bioactive glass composite scaffold are capable of promoting angiogenesis and supporting osteogenesis..

## 5. Conclusions

We have combined novel hypoxia-mimicking cobalt bioactive glasses with CG scaffolds optimised for bone repair. The results have demonstrated that these scaffolds may create a microenvironment capable of stimulating both angiogenesis and vascularisation via the release of cobalt, a known hypoxia mimic, as well as supporting osteogenesis as a result of the osteoinductive bioactive glass particles. Overall, this study indicates that an angiogenic response may be achievable through a growth factor-free biomaterials-based approach.

## Acknowledgements

The authors would like to thank the European Research Council (239685 - CollRegen -ERC-2009-STG) for providing financial support to this project and Integra Life Sciences Inc. for supplying collagen through a Materials Transfer Agreement.

## Figures

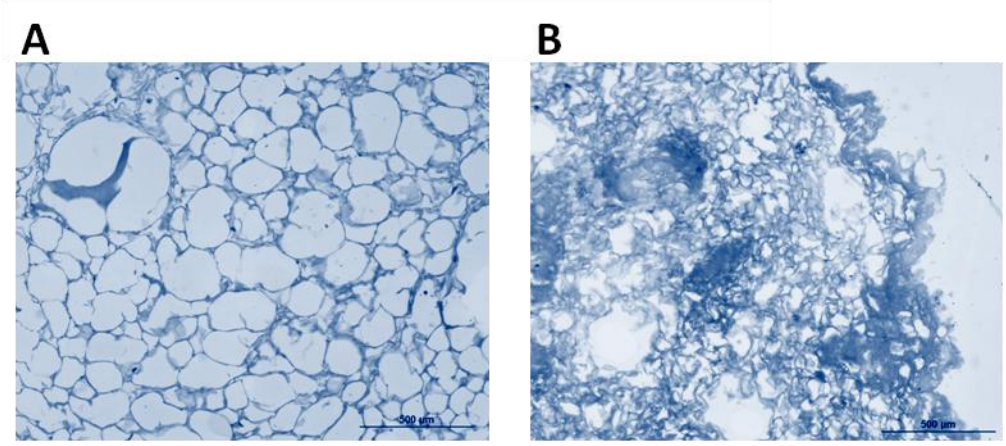


**Fig. 1** Pore structure of scaffolds. Toluidine Blue-stained images of cobalt bioactive glass/collagen–glycosaminoglycan scaffolds made at controlled freezing rates of **(A)** 1°C/min and **(B)** 4°C/min. A more homogenous pore structure for the composite scaffolds frozen at 1°C/min was demonstrated. Particles with a mean diameter of 100 μm were used. Scale bars, 500 μm.

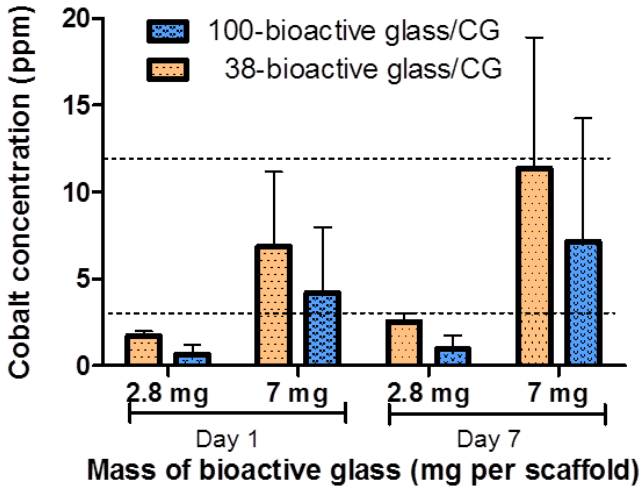


**Figure. 2**

**Fig. 2** Release of cobalt ions from the bioactive glass/collagen–glycosaminoglycan composites measured using Inductively Coupled Plasma-Mass Spectrometry (ICP-MS). The results show the release of cobalt after 24 h and the cumulative release at 7 days. Scaffolds incorporating 7 mg of bioactive glass per scaffold, released cobalt in the biologically active range of 3–12 ppm, which is the limit for HIF-1a activation (dashed lines).

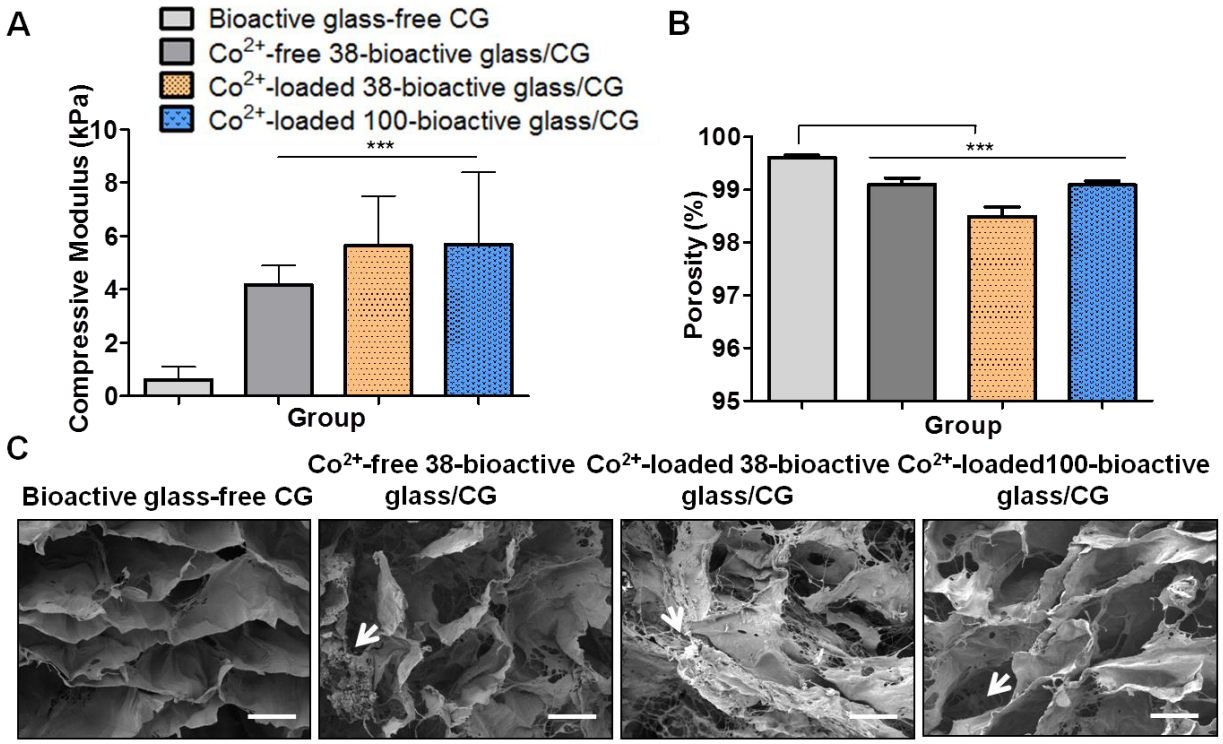


Figure. 3

**Fig. 3** Physical characterisation of bioactive glass/collagen–glycosaminoglycan (CG) scaffolds. **(A)** The addition of bioactive glass increases the compressive modulus of the scaffolds. Note that there is no significant difference in the stiffness with respect to the different types of bioactive glass. A concentration of 7 mg bioactive glass per scaffold was used. **(B)** Porosity of composites (7 mg bioactive glass per scaffold) was reduced compared with the bioactive glass-free CG scaffold, but was maintained at levels beneficial for cell and vascular infiltration. **(C)** Scanning electron micrographs of the bioactive glass-free CG scaffold and bioactive glass/CG scaffolds showing the incorporation of bioactive glass (white arrows) within the collagen matrix as well as the pore structure. Scale bars, 50 μm. *** $P$<0.001.

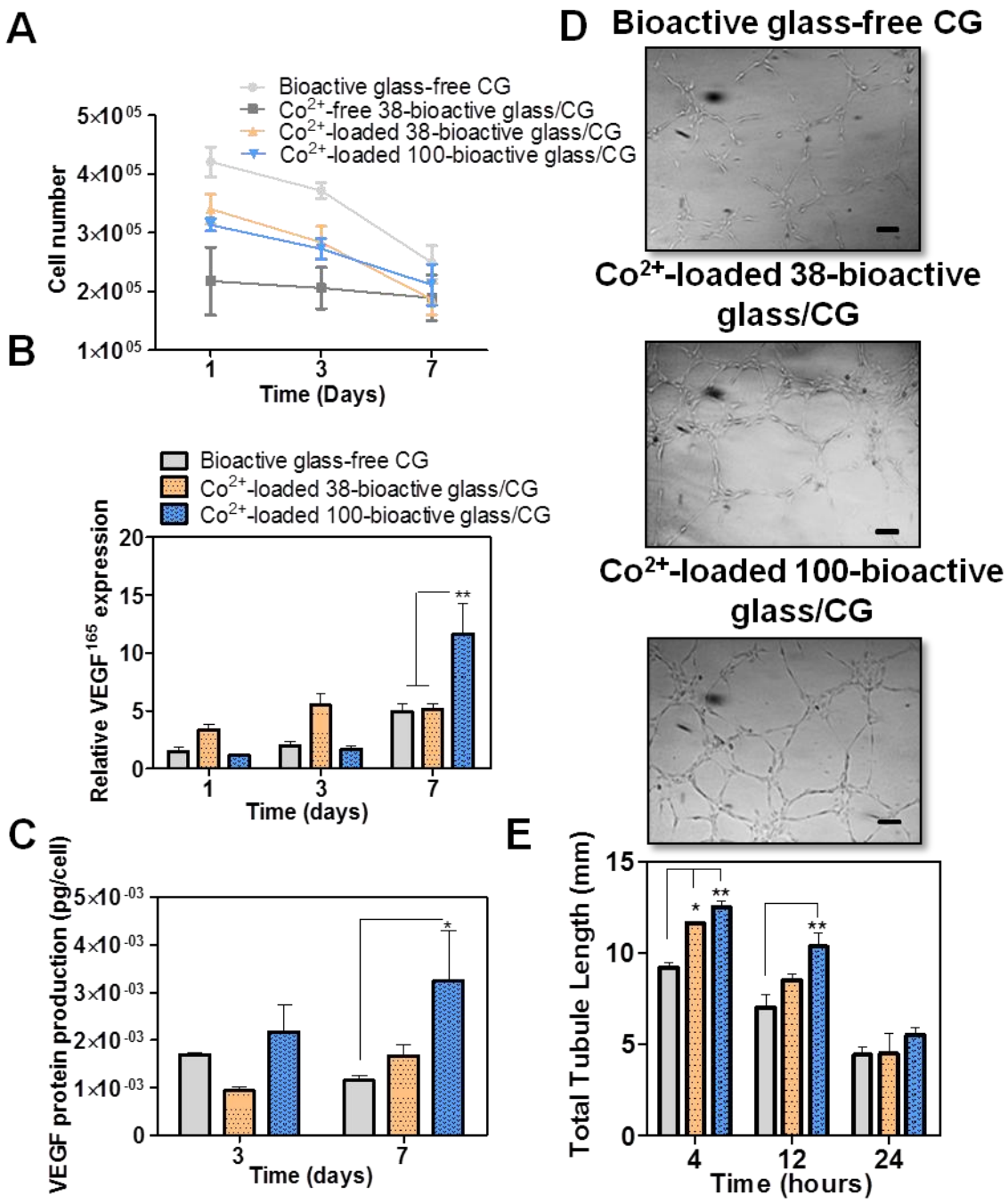


**Figure. 4**

**Fig. 4** Angiogenesis in bioactive glass/collagen–glycosaminoglycan (CG) scaffolds. **(A)** Number of endothelial cells on scaffolds at 1, 3 and 7 days post-seeding. An initial seeding density of 500,000 cells per scaffold was used. Cell numbers were initially higher in the bioactive glass-free CG scaffolds but were maintained at similar levels in all groups by 7 days. **(B)** Vascular Endothelial Growth Factor (VEGF) gene expression in HUVECs cultured on bioactive glass-free CG and bioactive glass-containing CG scaffolds at 1, 3 and 7 days. All data is normalized to the 24 h negative control (bioactive glass-free CG). **(C)** VEGF protein concentration in bioactive glass-containing CG composites seeded with HUVECs up to 7 days. There is a significant increase in concentration versus bioactive glass-free CG control at day 7. **(D)** Bright-field images of tubule formation. More mature networks are observed in

bioactive glass-containing CG scaffolds at 4 h. Scale bars, 100 µm. **(E)** Tubule length quantification showing that cobalt bioactive glass/CG scaffolds lead to enhanced tubule formation. * $P<0.05$; ** $P<0.01$.

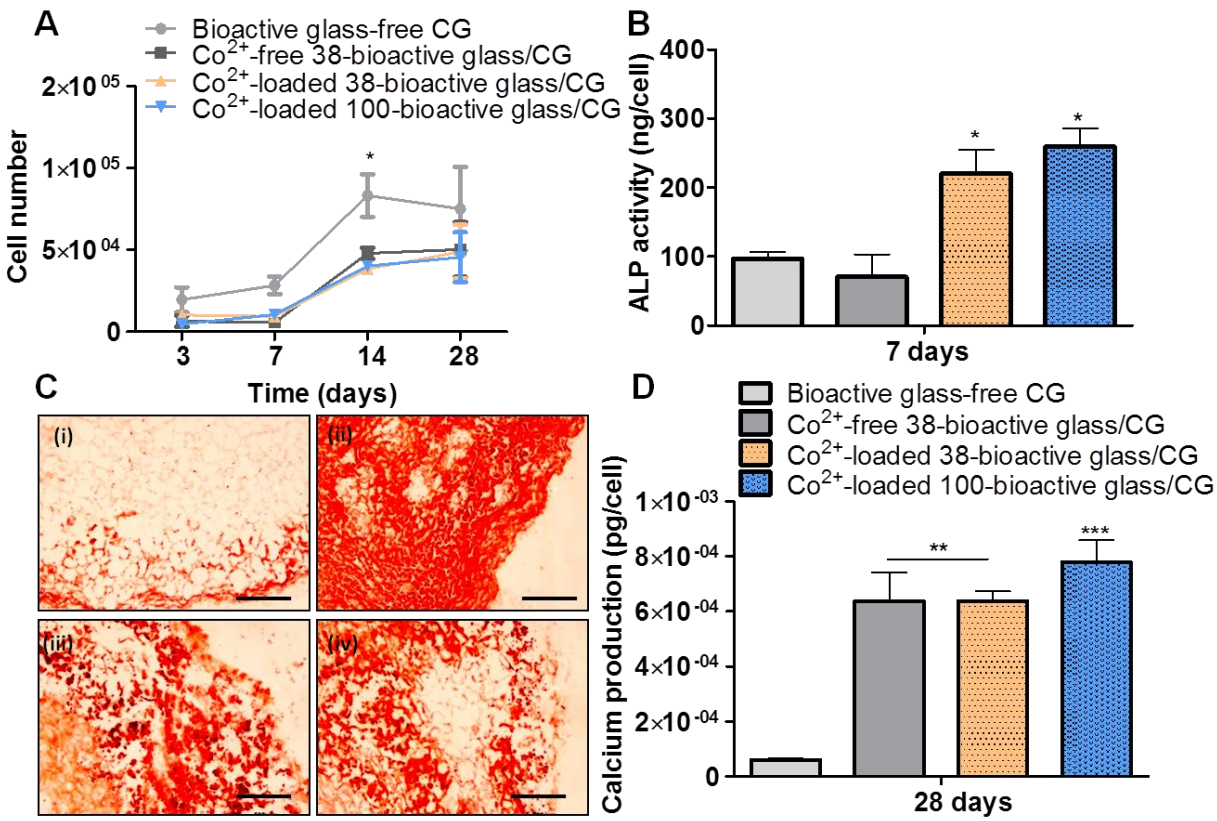


**Figure. 5**

**Fig. 5** Osteogenesis in bioactive glass/collagen–glycosaminoglycan (CG) scaffolds. **(A)** Increase in pre-osteoblast cell number on different scaffolds at days 3, 7, 14 and 28 compared with the CG scaffold with 38- and 100-µm-diameter cobalt bioactive glass particles. **(B)** Alkaline phosphatase activity increased in the presence of cobalt-eluting CG scaffolds compared with the bioactive glass-free CG scaffold and cobalt-free bioactive glass-containing scaffold. **(C)** Bright-field images of alizarin red-stained scaffolds demonstrating enhanced deposition in the bioactive glass-containing scaffolds relative to the bioactive glass-free control at 28 days (i). Staining was most intense for the cobalt-free bioactive glass-containing CG groups (ii), followed by the cobalt-eluting CG scaffolds (iii, iv) containing small and large-diameter bioactive glass particles. Scale bars, 500 µm. **(D)** There was an increase in calcium levels in the bioactive glass-containing CG scaffolds, the highest levels were seen in the group containing the larger-diameter bioactive glass particles. * $P<0.05$; ** $P<0.01$; *** $P<0.001$.

## Supplementary figure

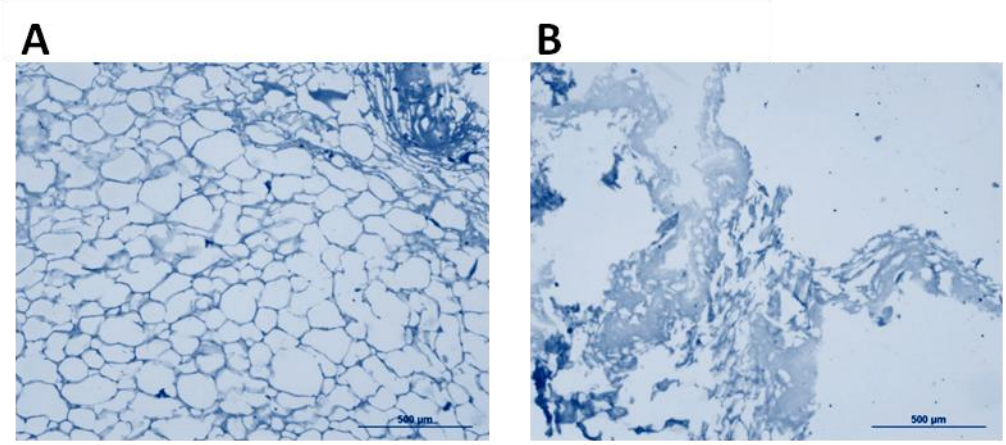


**Supplementary S1:** Pore structure of scaffolds. Toluidine Blue-stained images of cobalt bioactive glass/collagen–glycosaminoglycan scaffolds made by degassing the CG slurry prior to the addition of bioactive glass **(A)** and following the addition of BG **(B)** made at a controlled freezing rate of 1$^{o}$C/min. Composite scaffolds which were degassed prior to the addition of bioactive glass maintained their microstructural integrity and displayed a homogenous pore structure. Particles with a mean diameter of 100 µm were used. Scale bars, 500 µm.

## References

[1] Younger EM, Chapman MW. Morbidity at bone graft donor sites. Journal of orthopaedic trauma. 1989;3:192-5.
[2] Jones JR, Gentleman E, Polak J. Bioactive glass scaffolds for bone regeneration. Elements. 2007;3:393-9.
[3] Langer R, Vacanti JP. Tissue engineering. Science. 1993;260:920-6.
[4] O'Brien FJ, Harley BA, Yannas IV, Gibson L. Influence of freezing rate on pore structure in freeze-dried collagen-GAG scaffolds. Biomaterials. 2004;25:1077-86.
[5] O'Brien FJ. Biomaterials & scaffolds for tissue engineering. Mater Today. 2011;14:88-95.
[6] O'Brien FJ, Harley BA, Yannas IV, Gibson LJ. The effect of pore size on cell adhesion in collagen-GAG scaffolds. Biomaterials. 2005;26:433-41.
[7] Tierney CM, Jaasma MJ, O'Brien FJ. Osteoblast activity on collagen-GAG scaffolds is affected by collagen and GAG concentrations. Journal of biomedical materials research Part A. 2009;91:92-101.
[8] Lyons FG, Al-Munajjed AA, Kieran SM, Toner ME, Murphy CM, Duffy GP, et al. The healing of bony defects by cell-free collagen-based scaffolds compared to stem cell-seeded tissue engineered constructs. Biomaterials. 2010;31:9232-43.
[9] Alhag M, Farrell E, Toner M, Lee TC, O'Brien FJ, Claffey N. Evaluation of the ability of collagen-glycosaminoglycan scaffolds with or without mesenchymal stem cells to heal bone defects in Wistar rats. Oral Maxillofac Surg. 2012;16:47-55.

[10] Alhag M, Farrell E, Toner M, Claffey N, Lee TC, O'Brien F. Evaluation of early healing events around mesenchymal stem cell-seeded collagen-glycosaminoglycan scaffold. An experimental study in Wistar rats. Oral Maxillofac Surg. 2011;15:31-9.
[11] Hoppe A, Guldal NS, Boccaccini AR. A review of the biological response to ionic dissolution products from bioactive glasses and glass-ceramics. Biomaterials. 2011;32:2757-74.
[12] Maeno S, Niki Y, Matsumoto H, Morioka H, Yatabe T, Funayama A, et al. The effect of calcium ion concentration on osteoblast viability, proliferation and differentiation in monolayer and 3D culture. Biomaterials. 2005;26:4847-55.
[13] Gentleman E, Fredholm YC, Jell G, Lotfibakhshaiesh N, O'Donnell MD, Hill RG, et al. The effects of strontium-substituted bioactive glasses on osteoblasts and osteoclasts in vitro. Biomaterials. 2010;31:3949-56.
[14] Ahmed I, Parsons A, Jones A, Walker G, Scotchford C, Rudd C. Cytocompatibility and effect of increasing MgO content in a range of quaternary invert phosphate-based glasses. Journal of biomaterials applications. 2010;24:555-75.
[15] Hench LL. Genetic design of bioactive glass. J Eur Ceram Soc. 2009;29:1257-65.
[16] Novosel EC, Kleinhans C, Kluger PJ. Vascularization is the key challenge in tissue engineering. Advanced drug delivery reviews. 2011;63:300-11.
[17] Epstein NE. Pros, cons, and costs of INFUSE in spinal surgery. Surgical neurology international. 2011;2:10.
[18] Hamm A, Krott N, Breibach I, Blindt R, Bosserhoff AK. Efficient transfection method for primary cells. Tissue engineering. 2002;8:235-45.
[19] Trentin D, Hall H, Wechsler S, Hubbell JA. Peptide-matrix-mediated gene transfer of an oxygen-insensitive hypoxia-inducible factor-1alpha variant for local induction of angiogenesis. Proceedings of the National Academy of Sciences of the United States of America. 2006;103:2506-11.
[20] Malda J, Klein TJ, Upton Z. The roles of hypoxia in the In vitro engineering of tissues. Tissue engineering. 2007;13:2153-62.
[21] Buttyan R, Chichester P, Stisser B, Matsumoto S, Ghafar MA, Levin RM. Acute intravesical infusion of a cobalt solution stimulates a hypoxia response, growth and angiogenesis in the rat bladder. The Journal of urology. 2003;169:2402-6.
[22] Kim HH, Lee SE, Chung WJ, Choi Y, Kwack K, Kim SW, et al. Stabilization of hypoxia-inducible factor-1alpha is involved in the hypoxic stimuli-induced expression of vascular endothelial growth factor in osteoblastic cells. Cytokine. 2002;17:14-27.
[23] Schoubben A, Blasi P, Giovagnoli S, Rossi C, Ricci M. Development of a scalable procedure for fine calcium alginate particle preparation. Chemical Engineering Journal. 2010;160:363-9.
[24] Hu X, Yu SP, Fraser JL, Lu Z, Ogle ME, Wang JA, et al. Transplantation of hypoxia-preconditioned mesenchymal stem cells improves infarcted heart function via enhanced survival of implanted cells and angiogenesis. The Journal of thoracic and cardiovascular surgery. 2008;135:799-808.
[25] Azevedo MM, Jell G, O'Donnell MD, Law RV, Hill RG, Stevens MM. Synthesis and characterization of hypoxia-mimicking bioactive glasses for skeletal regeneration. J Mater Chem. 2010;20:8854-64.
[26] Azevedo MM, Tsigkou O, Nair R, Jell G, Jones J, Stevens M. HIF-stabilizing bioactive glasses for directing MSC behaviour. Tissue engineering Part A. 2014.
[27] Murphy CM, O'Brien FJ. Understanding the effect of mean pore size on cell activity in collagen-glycosaminoglycan scaffolds. Cell adhesion & migration. 2010;4:377-81.
[28] Tierney CM, Haugh MG, Liedl J, Mulcahy F, Hayes B, O'Brien FJ. The effects of collagen concentration and crosslink density on the biological, structural and mechanical properties of

collagen-GAG scaffolds for bone tissue engineering. Journal of the mechanical behavior of biomedical materials. 2009;2:202-9.
[29] Haugh MG, Jaasma MJ, O'Brien FJ. The effect of dehydrothermal treatment on the mechanical and structural properties of collagen-GAG scaffolds. Journal of biomedical materials research Part A. 2009;89:363-9.
[30] Street J, Bao M, deGuzman L, Bunting S, Peale FV, Jr., Ferrara N, et al. Vascular endothelial growth factor stimulates bone repair by promoting angiogenesis and bone turnover. Proceedings of the National Academy of Sciences of the United States of America. 2002;99:9656-61.
[31] Wan C, Gilbert SR, Wang Y, Cao X, Shen X, Ramaswamy G, et al. Activation of the hypoxia-inducible factor-1alpha pathway accelerates bone regeneration. Proceedings of the National Academy of Sciences of the United States of America. 2008;105:686-91.
[32] Livak KJ, Schmittgen TD. Analysis of relative gene expression data using real-time quantitative PCR and the 2(-Delta Delta C(T)) Method. Methods. 2001;25:402-8.
[33] Namiki A, Brogi E, Kearney M, Kim EA, Wu T, Couffinhal T, et al. Hypoxia induces vascular endothelial growth factor in cultured human endothelial cells. The Journal of biological chemistry. 1995;270:31189-95.
[34] Lieberman JR, Daluiski A, Einhorn TA. The role of growth factors in the repair of bone. Biology and clinical applications. The Journal of bone and joint surgery American volume. 2002;84-A:1032-44.
[35] Rahaman MN, Day DE, Bal BS, Fu Q, Jung SB, Bonewald LF, et al. Bioactive glass in tissue engineering. Acta biomaterialia. 2011;7:2355-73.
[36] Leu A, Leach JK. Proangiogenic potential of a collagen/bioactive glass substrate. Pharmaceutical research. 2008;25:1222-9.
[37] Cunniffe GM, Dickson GR, Partap S, Stanton KT, O'Brien FJ. Development and characterisation of a collagen nano-hydroxyapatite composite scaffold for bone tissue engineering. Journal of materials science Materials in medicine. 2010;21:2293-8.
[38] Gleeson JP, Plunkett NA, O'Brien FJ. Addition of hydroxyapatite improves stiffness, interconnectivity and osteogenic potential of a highly porous collagen-based scaffold for bone tissue regeneration. Eur Cell Mater. 2010;20:218-30.
[39] Wu C, Zhou Y, Fan W, Han P, Chang J, Yuen J, et al. Hypoxia-mimicking mesoporous bioactive glass scaffolds with controllable cobalt ion release for bone tissue engineering. Biomaterials. 2012;33:2076-85.
[40] Steinbrech DS, Mehrara BJ, Saadeh PB, Greenwald JA, Spector JA, Gittes GK, et al. VEGF expression in an osteoblast-like cell line is regulated by a hypoxia response mechanism. American journal of physiology Cell physiology. 2000;278:C853-60.
[41] Peters K, Unger RE, Barth S, Gerdes T, Kirkpatrick CJ. Induction of apoptosis in human microvascular endothelial cells by divalent cobalt ions. Evidence for integrin-mediated signaling via the cytoskeleton. Journal of materials science Materials in medicine. 2001;12:955-8.
[42] Stacker SA, Achen MG. The vascular endothelial growth factor family: signalling for vascular development. Growth Factors. 1999;17:1-11.
[43] Peng H, Usas A, Olshanski A, Ho AM, Gearhart B, Cooper GM, et al. VEGF improves, whereas sFlt1 inhibits, BMP2-induced bone formation and bone healing through modulation of angiogenesis. Journal of bone and mineral research : the official journal of the American Society for Bone and Mineral Research. 2005;20:2017-27.
[44] Semenza GL. Life with oxygen. Science. 2007;318:62-4.
[45] Shweiki D, Itin A, Soffer D, Keshet E. Vascular endothelial growth factor induced by hypoxia may mediate hypoxia-initiated angiogenesis. Nature. 1992;359:843-5.

[46] Gorustovich AA, Roether JA, Boccaccini AR. Effect of bioactive glasses on angiogenesis: a review of in vitro and in vivo evidences. Tissue Eng Part B Rev. 2010;16:199-207.
[47] Kent Leach J, Kaigler D, Wang Z, Krebsbach PH, Mooney DJ. Coating of VEGF-releasing scaffolds with bioactive glass for angiogenesis and bone regeneration. Biomaterials. 2006;27:3249-55.
[48] Matsiko A, Levingstone TJ, O'Brien FJ, Gleeson JP. Addition of hyaluronic acid improves cellular infiltration and promotes early-stage chondrogenesis in a collagen-based scaffold for cartilage tissue engineering. Journal of the mechanical behavior of biomedical materials. 2012;11:41-52.
[49] Hench LL, Polak JM. Third-generation biomedical materials. Science. 2002;295:1014-7.
[50] Jones JR, Tsigkou O, Coates EE, Stevens MM, Polak JM, Hench LL. Extracellular matrix formation and mineralization on a phosphate-free porous bioactive glass scaffold using primary human osteoblast (HOB) cells. Biomaterials. 2007;28:1653-63.
[51] Bergeron E, Marquis ME, Chretien I, Faucheux N. Differentiation of preosteoblasts using a delivery system with BMPs and bioactive glass microspheres. J Mater Sci-Mater M. 2007;18:255-63.
[52] Hattar S, Asselin A, Greenspan D, Oboeuf M, Berdal A, Sautier JM. Potential of biomimetic surfaces to promote in vitro osteoblast-like cell differentiation. Biomaterials. 2005;26:839-48.
[53] Xynos ID, Edgar AJ, Buttery LD, Hench LL, Polak JM. Gene-expression profiling of human osteoblasts following treatment with the ionic products of Bioglass 45S5 dissolution. Journal of biomedical materials research. 2001;55:151-7.
[54] Alcaide M, Portoles P, Lopez-Noriega A, Arcos D, Vallet-Regi M, Portoles MT. Interaction of an ordered mesoporous bioactive glass with osteoblasts, fibroblasts and lymphocytes, demonstrating its biocompatibility as a potential bone graft material. Acta biomaterialia. 2010;6:892-9.
[55] Patel ZS, Young S, Tabata Y, Jansen JA, Wong ME, Mikos AG. Dual delivery of an angiogenic and an osteogenic growth factor for bone regeneration in a critical size defect model. Bone. 2008;43:931-40.